中國機械工程學刊第四十一卷第四期第 427~439 頁(民國一百零九年)
Journal of the Chinese Society of Mechanical Engineers, Vol.41, No.4, pp 427~439 (2020)

# Numerical Analysis of Nitric Oxide Emission from a Sulfur Recovery Unit Thermal Reactor Using Rounded Corners, a Choke Ring or a Vector Wall

Chun-Lang Yeh*

**Keywords**：sulfur recovery unit, thermal reactor, nitrogen oxides, zone 1 corner geometry, choke ring, vector wall.

## ABSTRACT

Sulfur recovery unit (SRU) thermal reactor is important equipment in a sulfur plant. Its operating temperature can exceed 1600ºC and thus lead to the formation of nitrogen oxides (NOx). In this paper, NOx produced by an industrial-scale SRU thermal reactor is analyzed. Both the prototype reactor and its modifications, including modifying the zone 1 corner geometry, modifying the choke ring, and using a vector wall, are compared to seek a feasible way of reducing NOx emission. From the simulation results, it is found that the SRU thermal reactor with a radius of curvature 1m at the zone 1 corner has the lowest nitric oxide (NO) emission among the radii of curvature at the zone 1 corner investigated. Among the choke ring heights investigated, the SRU thermal reactor having a choke ring height of 1.11m has the highest NO emission while the one having a choke ring height of 0.74m has a lower NO emission. Further, among the choke ring positions investigated, the SRU thermal reactor having a choke ring away from the zone 1 corner by 6m has the lowest NO emission while the one having a choke ring away from the zone 1 corner by 3m has the highest NO emission. The NO concentration at the reactor exit using a vector wall is higher than that using a choke ring. Among the SRU thermal reactors investigated in this study, the one without a choke ring has the lowest NO emission. However, it has the highest zone 2 temperature and this is harmful to the downstream heat exchanger tubes. Although a vector wall produces more sulfur, its NO emission is also higher. In summary, a SRU thermal reactor using a choke ring of 0.74m in height and 6m away from the zone 1 corner is a feasible compromise among the sulfur production, the operating temperature (service life consideration) and the NO emission.

*Paper Received October, 2018. Revised March, 2019, Accepted March, 2019, Author for Correspondence: Chun-Lang Yeh.*

* *Professor, Department of Aeronautical Engineering, National Formosa University, Huwei, Yunlin,, Taiwan 63208, ROC.*

## INTRODUCTION

NOx is a pollutant. It is one of the major sources of air pollution. NOx is a precursor for photochemical smog, contributes to acid rain and causes ozone depletion. In addition, NOx has been recognized as one of the major causes of excessive peroxide concentration in the atmosphere. NOx control has become a worldwide problem. The formation of NOx can be attributed to four distinct chemical kinetic processes: thermal NOx, prompt NOx, fuel NOx and intermediate $N_2O$. In general, the contribution from prompt NOx and intermediate $N_2O$ is minor. Fuel NOx is produced by oxidation of nitrogen atoms contained in nitrogen-bearing fuels. Thermal NOx is formed by the oxidation of atmospheric nitrogen molecules present in the combustion air and is strongly dependent on the temperature. Considering the fuel composition shown in Table 1 for this study, thermal NOx is the major source of NOx. NOx emission consists of mostly nitric oxide (NO) (around 95%) and to a lesser degree nitrogen dioxide ($NO_2$) and nitrous oxide ($N_2O$) (around 5%). Therefore, the NO species is the major concern in this study.

Table 1. The design conditions at the acid gas inlet holes and the air inlet hole.

| Oxygen-Normal Supply | | | |
|---|---|---|---|
| | Acid Gas to Zone 1 | Acid Gas to Zone 2 | Air Inlet |
| Species | *x* (%) | | |
| $O_2$ | 0 | 0 | 19.87 |
| $N_2$ | 0 | 0 | 74.98 |
| $H_2O$ | 7.83 | 4.12 | 5.15 |
| $CO_2$ | 1.27 | 1.5 | 0 |
| $H_2S$ | 82.06 | 89.88 | 0 |

| | | | |
|---|---|---|---|
| $CH_4$ | 2.28 | 2.7 | 0 |
| $C_2H_6$ | 1.52 | 1.8 | 0 |
| $NH_3$ | 5.04 | 0 | 0 |
| $T$ (K) | 319.92 | 316.15 | 403.15 |
| $P$ ($N/m^2$) | 76,920 | 75,068 | 74,382 |
| $V$ (m/s) | 11.62 | 2.08 | 12.4 (Radial) |
| | | | 34.1 (Tangential) |

| Oxygen-Rich Supply | | | |
|---|---|---|---|
| | Acid Gas to Zone 1 | Acid Gas to Zone 2 | Air Inlet |
| Species | $x$ (%) | | |
| $O_2$ | 0 | 0 | 23.85 |
| $N_2$ | 0 | 0 | 71.26 |
| $H_2O$ | 4.12 | 27.97 | 4.89 |
| $CO_2$ | 1.48 | 0 | 0 |
| $H_2S$ | 89.9 | 39.61 | 0 |
| $CH_4$ | 2.7 | 0 | 0 |
| $C_2H_6$ | 1.8 | 0 | 0 |
| $NH_3$ | 0 | 32.42 | 0 |
| $T$ (K) | 313.15 | 316.15 | 397.15 |
| $P$ ($N/m^2$) | 75,068 | 75,068 | 89,572 |
| $V$ (m/s) | 11.46 | 1.88 | 10.8 (Radial) |
| | | | 29.8 (Tangential) |

SRU thermal reactor is the most important equipment in a sulfur plant. It converts the ammonia ($NH_3$), hydrogen sulfide ($H_2S$) and hydrocarbons in the reactants into sulfur. Most of the sulfur elements are recovered from the SRU thermal reactor. The first section of a SRU that uses the Claus process is composed of a burner, a thermal reactor and a waste heat exchanger. The configuration and dimensions of the first section of a SRU for a typical petroleum refinery are shown in Fig.1.

There have been theoretical and experimental studies of SRU thermal reactors. Adewale et al. (2016) studied the thermal decomposition of $H_2S$ into hydrogen and sulfur. Using the net fraction of the acid gas feed to the cracking coils as the controlling parameter, its effect on the hydrogen production, the thermal reactor's energy requirement, the stability of the burner flame, the steam production, the temperature of a Claus reactor and the sulfur recovery of the SRU were studied. Chardonneaua et al. (2015) presented experimental and simulation results for the addition of various amounts of toluene or carbon dioxide/toluene mixtures into the $H_2S$ gas stream. The role of the operating temperature of the reactor was also studied. The results showed that there is a decrease in conversion efficiency when the amount of toluene or carbon dioxide/toluene added to the $H_2S$ gas stream increases. The addition of toluene increases the optimum reactor temperature for enhanced sulfur recovery, but the presence of $CO_2$ reduces the optimum operating temperature. Selim et al. (2013) examined the quality of sulfur deposits that were collected from $H_2S$ combustion. Sulfur deposits from $H_2S$ combustion under various conditions were captured and analyzed using X-ray powder diffraction and laser induced breakdown spectroscopy diagnostics. Monnery et al. (2000) experimentally studied the reaction between $H_2S$ and

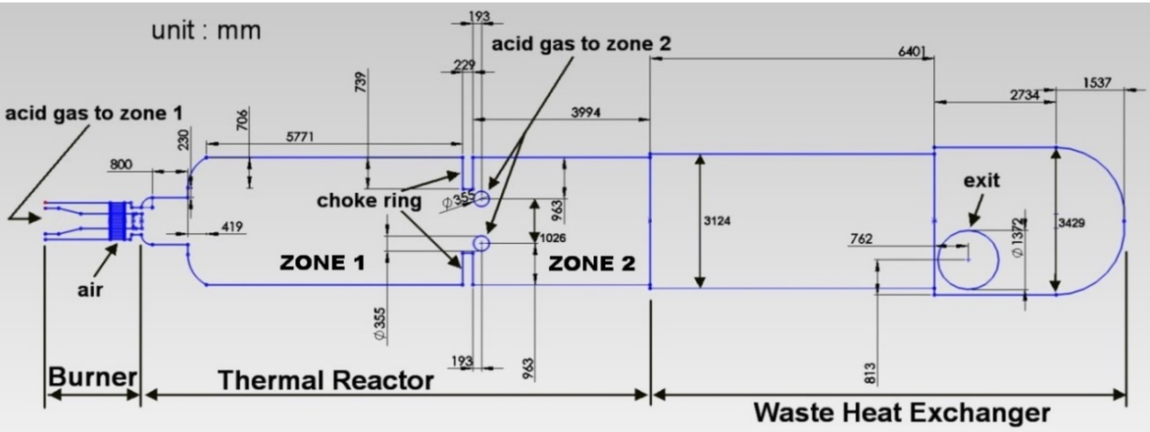


(a) the overall view

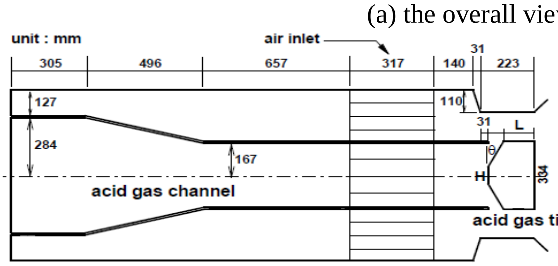


(b) enlarged view for the burner section

Fig. 1. The configuration and dimensions of the first section of a SRU.

$SO_2$ using practical Claus thermal reactor temperatures between 850 and 1150°C and residence times between 0.05 and 1.2 seconds. The kinetic data obtained were used to develop a new reaction rate expression.

NOx is produced in a SRU thermal reactor when the operating temperature exceeds 1600°C. In addition, SRU thermal reactors are negatively affected by high temperature operations because high temperature can damage the refractory and the heat exchanger tubes. Our experience of operating a practical SRU thermal reactor in Taiwan showed that the refractories at the zone 1 corner and the choke ring are the parts of a thermal reactor that experience the greatest deterioration. The zone 1 corner has a suddenly expanded geometry and a recirculation zone forms behind it. The temperature at the zone 1 corner can exceed the maximum service temperature of the refractory and cause collapse or deformation. The choke ring is subjected to a bending moment from the rapid combustion gas stream and can collapse or deform.

The flow field in a SRU thermal reactor involves many complicated mechanisms, such as turbulent mixing, convection and radiation heat transfer modes, combustion, as well as NOx and SOx (sulfur oxides) formations. These mechanisms are all highly complex and may interact with each other and thus makes the analysis much more difficult. There have been no researches discussing pollutants produced by SRU thermal reactors in existing literatures. However, there are many theoretical and experimental studies discussing pollutants produced by other industrial heating equipment. Hassan et al. (2009) simulated the combustion process occurring in the combustion chamber of some domestic boilers. A two-dimensional computational fluid dynamics (CFD) model is established to simulate the combustion chamber domain and the partially premixed combustion model with a postprocessor for NOx calculations is used to simulate the combustion process inside the combustion chamber. The concept of changing the mixture inlet velocity is found to be an effective method to improve the design of the burner in order to reduce the pollutant emissions produced from the boiler with no effect on the boiler efficiency. Franco and Diaz (2009) described the state of the art in the field of ‘‘clean coal technologies’’ showing the perspectives of improvement and the critical elements. They reviewed and analyzed the emission control of NOx, SOx and particle matter as well as advanced coal conversion pathways such as ultra-supercritical (USC), pressurized fluidized bed combustion (PFBC) and integrated gasification combined cycle (IGCC). The paper also outlined some aspects of carbon dioxide emission control strategies. Normann et al. (2009) reviewed available techniques for controlling both the emission of NOx to the atmosphere and the content of NOx in the captured carbon dioxide. They indicated that for a first generation of oxy-fuel power plants, conventional primary NOx control should be sufficient to meet today’s emission regulations, if based on emission per unit of fuel supplied. However, there are several opportunities for new methods of NOx control in oxy-fuel plants, depending on future emission and storage legislation for carbon capture schemes. Shin et al. (2007) developed a comprehensive computer program to evaluate the efficiency of a selective non-catalytic reduction (SNCR) system for a boiler. The standard $k$-$\varepsilon$ turbulence model and the eddy breakup model were incorporated to analyze the Reynolds stresses and the turbulent reaction of major fuel species, respectively. Their calculations showed that the removal efficiency of NO was significantly improved by increasing penetration depth of the reducing agent into the center region of boiler. Javed et al. (2007) presented a review of NOx removal techniques with particular reference to SNCR technology. A review of various features related to selective non-catalytic gas phase injection of ammonia and ammonium salts (as reducing agent) was presented. CFD modeling was also applied to SNCR. In addition, a two-stage NOx removal strategy to control un-reacted ammonia slip and to improve overall efficiency was discussed and a summary highlighted various areas needing further research was given.

In this paper, NO emissions from industrial-scale SRU thermal reactors (both a prototype reactor and its modifications, including modifying the zone 1 corner geometry, modifying the choke ring, and using a vector wall) are analyzed and compared. Practical operating conditions from a petrochemical corporation in Taiwan were used as the design conditions for the discussion. Note that the removal of NOx is facilitated in other equipment and therefore is not discussed in this paper. This research is focused on the comparison of NO emission by SRU thermal reactors to seak a feasible way of reducing NO emission.

## NUMERICAL METHODS AND PHYSICAL MODELS

In this study, the ANSYS FLUENT V.17.0.2 commercial code is used to simulate the reaction and fluid flow in a SRU thermal reactor. The SIMPLE algorithm by Patankar (1980) is used to solve the governing equations. The discretizations of convection terms and diffusion terms are performed using the power-law scheme and the central difference scheme, respectively. In terms of physical models, considering the accuracy and stability of the models and the evaluations of other researchers, the standard *k-ε* Model (Launder and Spalding, 1972), the P-1 radiation model (Siegel and Howell, 1992) and the non-premixed combustion model with β–type probability density function (Sivathanu and Faeth, 1990) are used for the turbulence, radiation and combustion simulations, respectively. The standard wall functions (Launder and Spalding, 1974) are used to resolve the flow quantities (velocity, temperature and turbulence quantities) at the near-wall regions. The detailed governing equations and convergence criterion were described in previous studies by the author (Yeh, 2013, 2016a).

In this study, the numerical model of a SRU thermal reactor is constructed using an unstructured grid. Fig.2 shows the numerical model of the prototype SRU thermal reactor. In Fig.2, the heat exchanger section consists of 19 tubes. Each tube has a diameter of 0.5m, as shown schematically in Fig.3. The heat absorption rate for each heat exchanger tube is 40,000 W/m$^2$ and the other walls are adiabatic. No slip condition is applied on any of the solid walls. The exit of the heat exchanger section is connected to other equipment at 300 K and 1 atm by a pipe that is 1.372m in diameter and 11.5m in length.


Fig. 2. The numerical model for the SRU thermal reactor investigated.

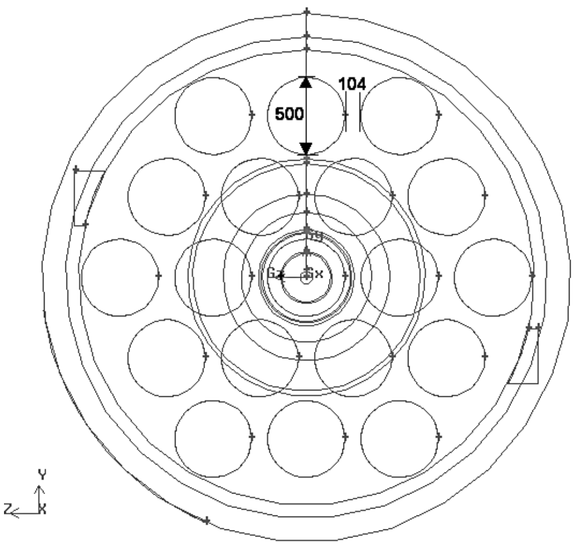


Fig. 3. An illustration of the arrangement of heat exchanger tubes.

In this study, two types of oxygen supplies are investigated: an oxygen-normal supply and an oxygen-rich supply. An oxygen-rich supply increases sulfur recovery. The design conditions (including the species compositions, the temperature, the pressure and the velocity) at the acid gas inlet holes of zone 1 and zone 2 and at the air inlet hole are listed in Table 1, and are used as the boundary conditions. These conditions are practical operating conditions that are used by a petrochemical corporation in Taiwan. The turbulence kinetic energy is 10% of the inlet mean flow kinetic energy and the turbulence dissipation rate is computed using Eq.(1).

$$\varepsilon = C_{\mu}^{3/4}\frac{k^{3/2}}{l}\ . \tag{1}$$

where $l$=0.07L and L is the hydraulic diameter.

The grid independence test and the validation of numerical methods have been performed in a previous study by the author (Yeh, 2016a).

## RESULTS AND DISCUSSION

### Effect of Zone 1 Corner Geometry

With a rounded zone 1 corner, the corner recirculation zone in zone 1 becomes smaller due to the streamlining effect of the rounded corner, and this can reduce the temperature. However, the temperature may also be increased due to the compression effect caused by the decreased volume in zone 1. These two effects (the smaller corner recirculation zone and the compression effect) lead to an optimal radius of curvature at the zone 1 corner. In this study, nine different radii of curvature at the zone 1 corner, including 0m (without rounded corners, i.e. the prototype reactor), 0.5m, 1m, 1.5m, 2m, 2.5m, 3m, 3.5m and 4m, are calculated to investigate the geometric effects of the zone 1 corner. Fig.4 shows the numerical models of SRU thermal reactors with different radii of curvature at the zone 1 corner.

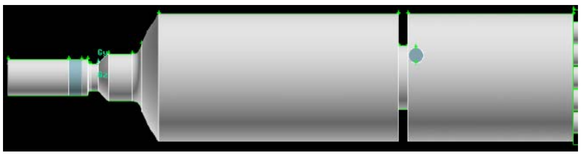

(a) without rounded corners (prototype reactor)

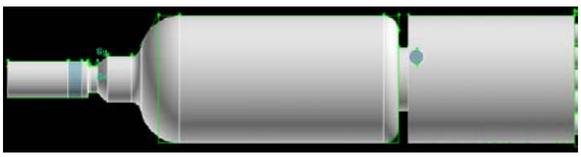

(b) with a radius of curvature 1m

(c) with a radius of curvature 2m

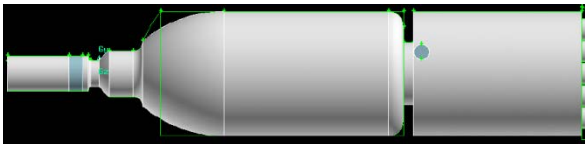

(d) with a radius of curvature 3m

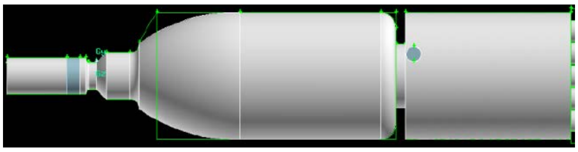

(e) with a radius of curvature 4m

Fig. 4. Numerical models of a SRU thermal reactor with different radii of curvature at the zone 1 corner.

Fig.5 shows the peak temperatures for SRU thermal reactors with different radii of curvature at the zone 1 corner. As stated above, there exists an optimal radius of curvature at the zone 1 corner for the temperature to be the lowest. It can be seen that the lowest peak temperature is obtained using a radius of curvature 1m at the zone 1 corner.

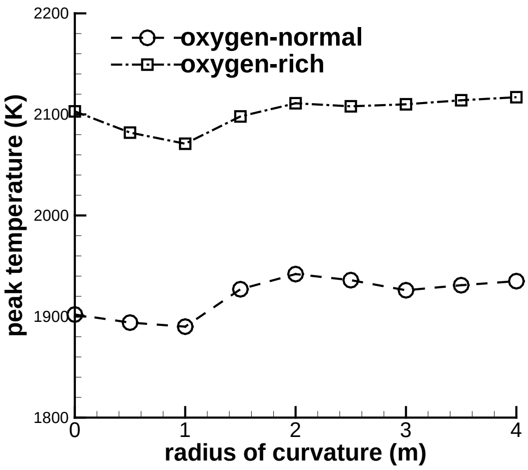


**Fig. 5.** Peak temperatures for SRU thermal reactors with different radii of curvature at the zone 1 corner.

Fig.6 shows the NO concentrations at the exit for SRU thermal reactors with different radii of curvature at the zone 1 corner. It is observed that the SRU thermal reactor with a radius of curvature 1m at the zone 1 corner has the lowest NO emission because of its lowest temperature. Figure 7 shows the temperature profiles for the SRU thermal reactor using a radius of curvature 1m at the zone 1 corner (Yeh, 2016b).

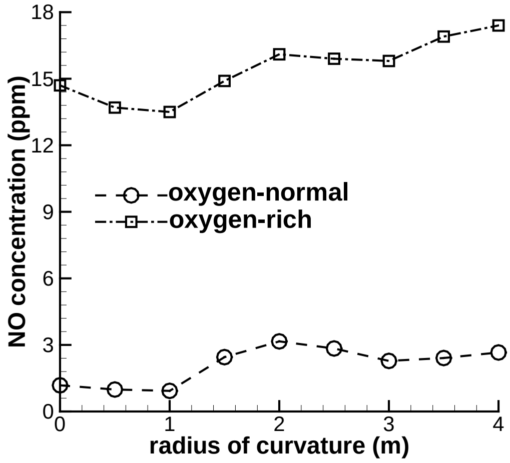


Fig. 6. NO concentrations at the exit for SRU thermal reactors with different radii of curvature at the zone 1 corner.

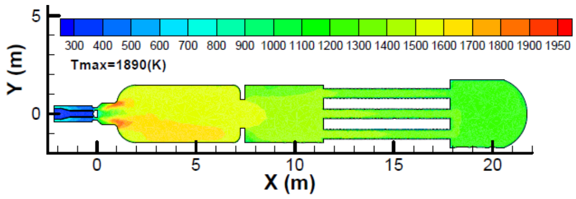


(a) oxygen-normal supply

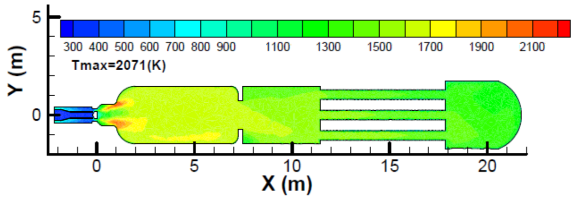


(b) oxygen-rich supply

Fig. 7. Temperature profiles for the SRU thermal reactor using a radius of curvature 1m at the zone 1 corner (Yeh, 2016b)

**Effect of a Choke Ring**

The interior of a SRU thermal reactor is divided into two zones by a choke ring. Temperature decreases across a choke ring because the thermal energy is converted into kinetic energy due to local flow acceleration. The zone in front of the choke ring (zone 1) is a higher temperature region while the zone behind the choke ring (zone 2) is a lower temperature region. A choke ring increases the residence time of fluid flow and therefore enhances chemical reaction. In addition, a choke ring acts as a shield against the radiation from zone 1 and thus protects the waste heat exchanger tubes from thermal damage. However, a choke ring is subjected to the stresses and moments caused by the rapidly moving combustion stream and the high temperature in zone 1. Therefore, it may collapse or deform.

Four different choke ring heights, including 0m (i.e. without a choke ring), 0.37m, 0.74m (i.e. the prototype reactor) and 1.11m, are calculated to investigate the effect of choke ring height on the NO emission. Fig.8 shows the numerical models of the SRU thermal reactors using different choke ring heights.

(a) without a choke ring

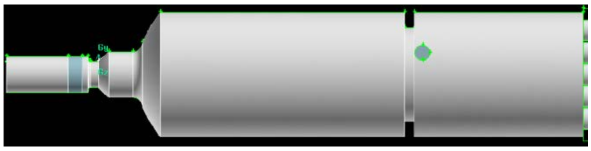

(b) using a choke ring of 0.37m in height

(c) using a choke ring of 0.74m in height

(d) using a choke ring of 1.11m in height

Fig. 8. Numerical models of the SRU thermal reactors using different choke ring heights.

From a previous study by the author (Yeh, 2016c) (or refer to Fig.9), it has been found that without a choke ring, the temperature difference between zone 1 and zone 2 is smaller, i.e. the temperature in zone 1 is lower while the temperature in zone 2 is higher in comparison with that having a choke ring. Note that a higher zone 2 temperature might be harmful to the downstream heat exchanger tubes. Further, the reactor without a choke ring has the lowest zone 1 average temperature while the reactor using a choke ring of 0.74m in height has the lowest peak temperature. On the other hand, with a choke ring height of 1.11m, the blockage effect of the choke ring leads to the highest zone 1 average temperature (Yeh, 2016c).

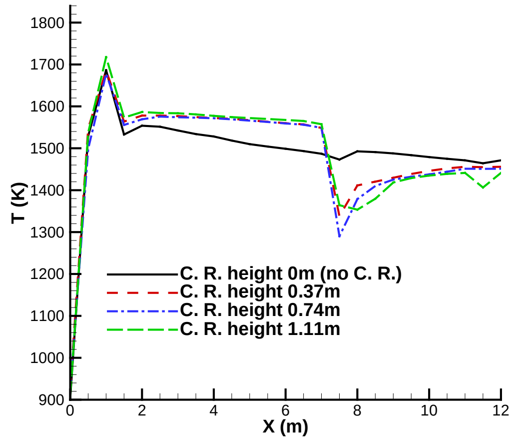


(a) oxygen-normal supply

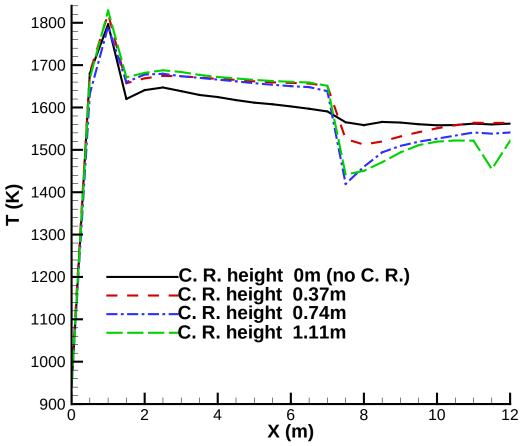


(b) oxygen-rich supply

Fig. 9. Comparison of cross-sectional average temperature for SRU thermal reactor using different choke ring heights (Yeh, 2016c).

Table 2 shows the NO concentrations at the exit for SRU thermal reactors using different choke ring heights. It can be seen that the SRU thermal reactor without a choke ring has the lowest NO emission because of its lowest zone 1 temperature. However, its sulfur concentration at the exit is also the lowest from a previous study by the author (Yeh, 2016c). On the other hand, the SRU thermal reactor using a choke ring of 1.11m in height has the highest NO emission because of its highest zone 1 temperature. The SRU thermal reactor using a choke ring of 0.74m in height has a lower NO emission than those using choke ring heights of 0.37m or 1.11m. In addition, the SRU thermal reactor using a choke ring of 0.74m in height has the highest sulfur concentration at the exit from a previous study by the author (Yeh, 2016c).

Table 2. NO concentrations (ppm) at the exit for SRU thermal reactors using different choke ring heights.

| choke ring height (m) | 0 | 0.37 | 0.74 | 1.11 |
|---|---|---|---|---|
| oxygen-normal | 0.98 | 1.26 | 1.18 | 1.34 |
| oxygen-rich | 12.2 | 15.7 | 14.7 | 16.1 |

In the following discussion, five different choke ring positions (away from the zone 1 corner by 3m, 4m, 5m, 6m and 7m) are calculated to investigate the effects of choke ring positions on the NO emission. Fig.10 shows the numerical models of the SRU thermal reactor with a choke ring at different locations. The height of the choke ring is kept at 0.74m.

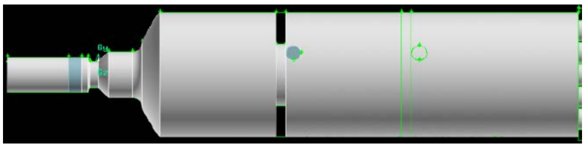

(a) choke ring away from zone 1 corner by 3m

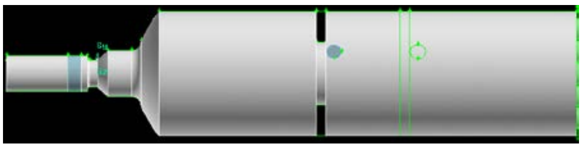

(b) choke ring away from zone 1 corner by 4m

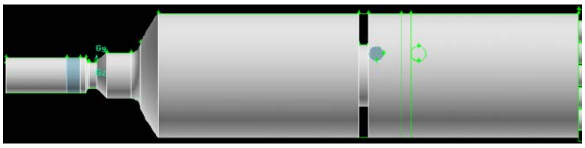

(c) choke ring away from zone 1 corner by 5m

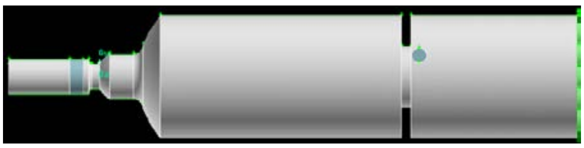

(d) choke ring away from zone 1 corner by 6m

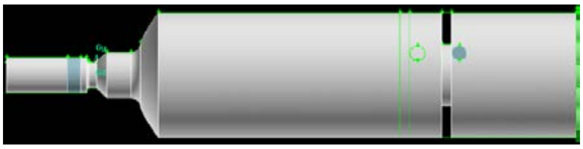

(e) choke ring away from zone 1 corner by 7m

Fig. 10. Numerical models of the SRU thermal reactor with a choke ring at different locations.

From a previous study by the author (Yeh, 2015) (or refer to Fig.11), it has been found that a larger zone 1 leads to a larger higher temperature region, as shown in Fig.11. Although a smaller zone 1 leads to a smaller higher temperature region, the peak temperature is not necessarily lower. On the contrary, for a smaller zone 1, the peak temperature may be higher due to the compression effect of a smaller region. There exists an optimal location of the choke ring for the peak temperature to be the lowest. It was found from a previous study by the author (Yeh, 2015) that the reactor with a choke ring away from the zone 1 corner by 6m has the lowest peak temperature.

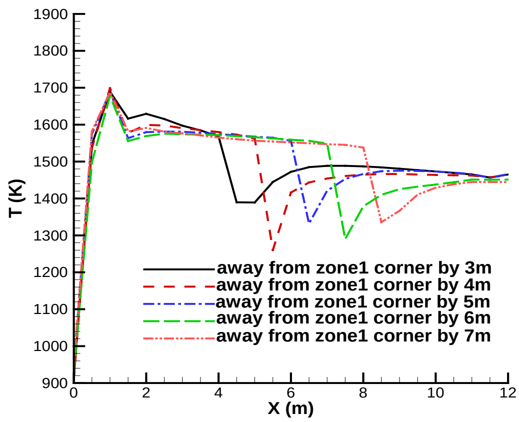


(a) oxygen-normal supply

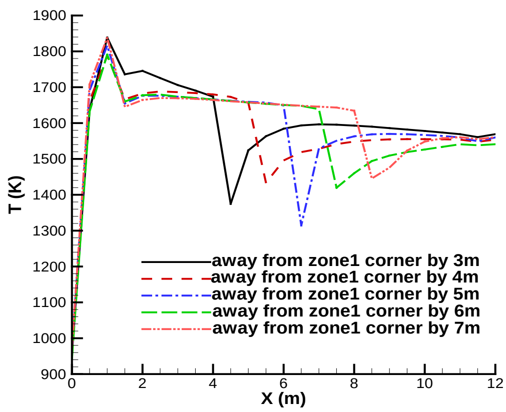


(b) oxygen-rich supply

Fig. 11. Comparison of cross-sectional average temperatures for SRU thermal reactors using choke rings at different locations (Yeh, 2015).

Table 3 shows the NO concentrations at the exit for SRU thermal reactors using choke rings at different locations. It can be observed that the SRU thermal reactor with a choke ring away from the zone 1 corner by 6m has the lowest NO emission because of its lowest peak temperature. On the other hand, the SRU thermal reactor with a choke ring away from the zone 1 corner by 3m has the highest NO emission because of its highest zone 1 average temperature.

Table 3. NO concentrations (ppm) at the exit for SRU thermal reactors using choke rings at different locations.

| distance away from zone 1 corner (m) | 3 | 4 | 5 | 6 | 7 |
|---|---|---|---|---|---|
| oxygen-normal | 1.69 | 1.46 | 1.31 | 1.18 | 1.54 |
| oxygen-rich | 18.2 | 16.7 | 15.5 | 14.7 | 17.1 |

**Effect of a Vector Wall**

The specific arrangement of the holes of a vector wall results in spiral motion or flow impingement behind the vector wall and thereby enhances mixing and temperature uniformity. Fig.12 shows the numerical models of SRU thermal reactors using a choke ring or a vector wall. The choke ring or the vector wall is located at 6m away from the zone 1 corner. Two kinds of vector walls are investigated, including an opposing-type vector wall and a spiral-type vector wall. The holes of an opposing-type vector wall are arranged in a manner that exits of the upper half and the lower half of holes are in opposite directions that produce flow impingement behind the vector wall while the holes of a spiral-type vector wall are arranged in a spiral manner that yields spiral motion behind the vector wall. Both the opposing-type and the spiral-type vector walls can enhance mixing and temperature uniformity. However, their larger blockage effects due to larger solid surface area also increase the temperature in front of the vector walls.

(a) using a choke ring

(b) using a vector wall

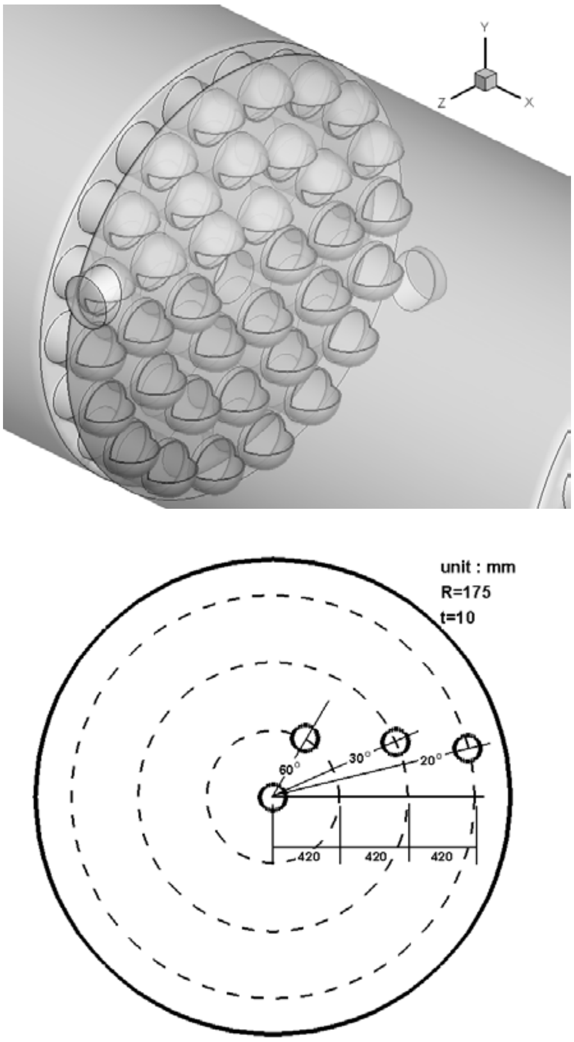

(c) enlarged view and arrangement of an opposing-type vector wall

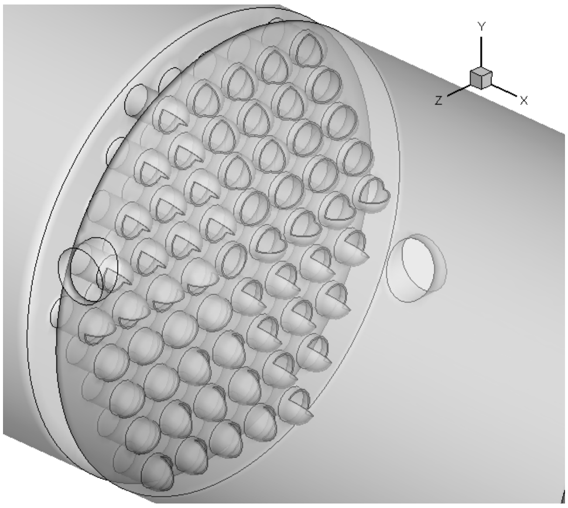


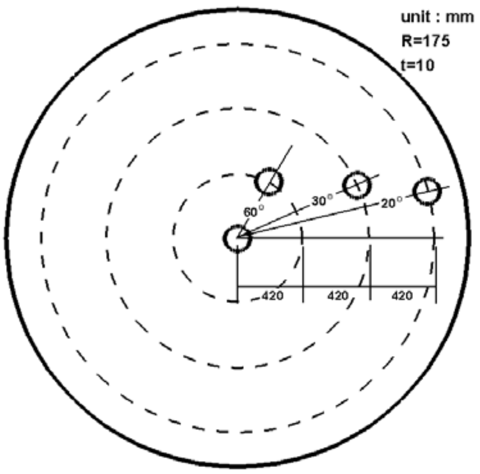


(d) enlarged view and arrangement of a spiral-type vector wall

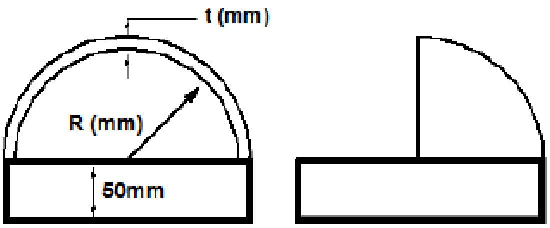


(e) configuration and dimension of the hole of a vector wall

Fig. 12. Numerical models of SRU thermal reactors using a choke ring or a vector wall.

From a previous study by the author (Yeh, 2018) (or refer to Fig.13), it was found that the average temperature in zone 2 is increased using a vector wall. In addition, the larger solid surface area of a vector wall results in a larger blockage effect and therefore the average temperature in zone 1 is also increased. In a practical SRU thermal reactor, the refractory may be ruptured due to high temperature, for example, near the zone 1 corner. It is observed from Fig.13 that the temperature across a vector wall becomes more uniform due to better mixing. The spiral-type arrangement produces a higher cross-sectional average temperature than the opposing-type arrangement. Among the choke ring and vector walls investigated, the spiral-type vector wall produces the best mixing effect and therefore results in the highest average temperature.

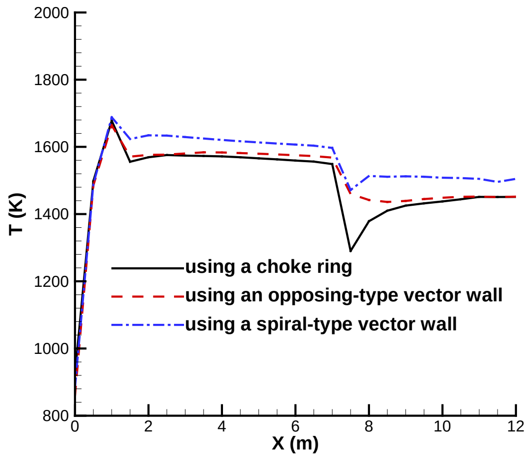


(a) oxygen-normal supply

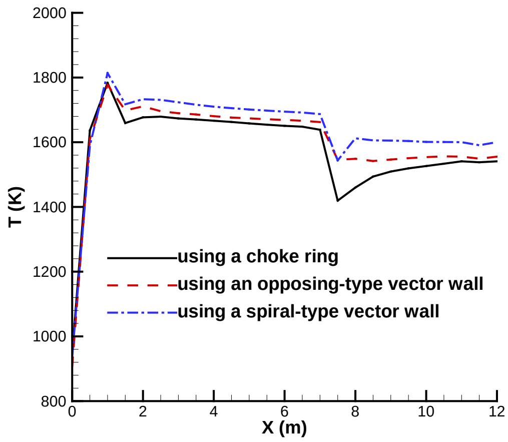


(b) oxygen-rich supply

Fig. 13. Comparison of cross-sectional average temperatures for the SRU thermal reactors using a choke ring or a vector wall (Yeh, 2018).

Figure 14 shows the temperature profiles for the SRU thermal reactors using a spiral-type vector wall (Yeh, 2016b). It is observed that the temperature across a vector wall becomes more uniform due to better mixing. Figure 15 shows the stream traces for the SRU thermal reactors using a choke ring or a spiral-type vector wall (Yeh, 2016b). The spiral motion behind the vector wall is clearly observed.

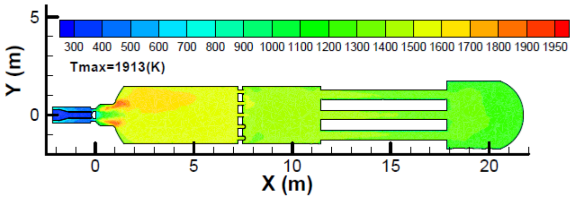


(a) oxygen-normal supply

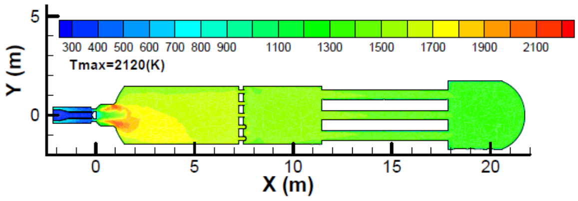


(b) oxygen-rich supply

Fig. 14. Temperature profiles for the SRU thermal reactors using a vector wall (Yeh, 2016b).

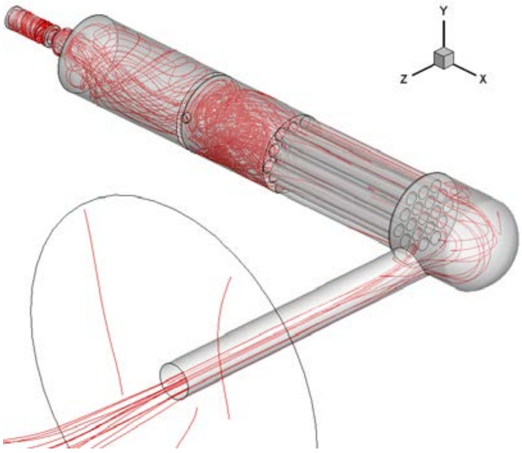


(a) using a choke ring (oxygen-normal supply)

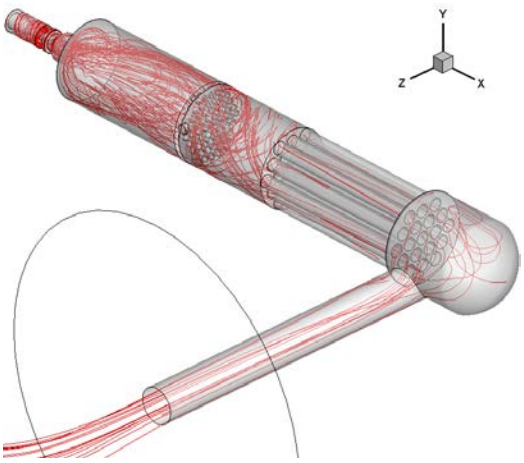


(b) using a vector wall (oxygen-normal supply)

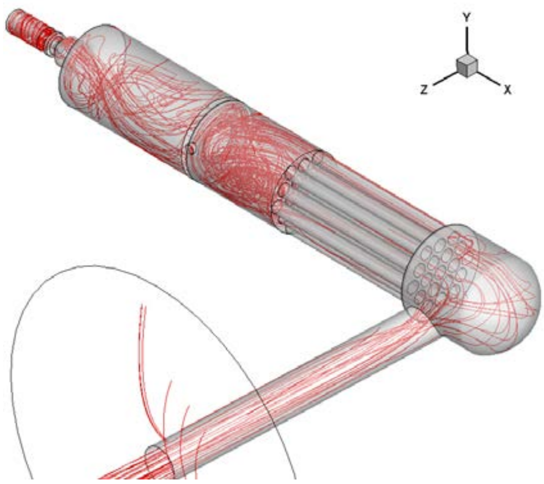


(c) using a choke ring (oxygen-rich supply)

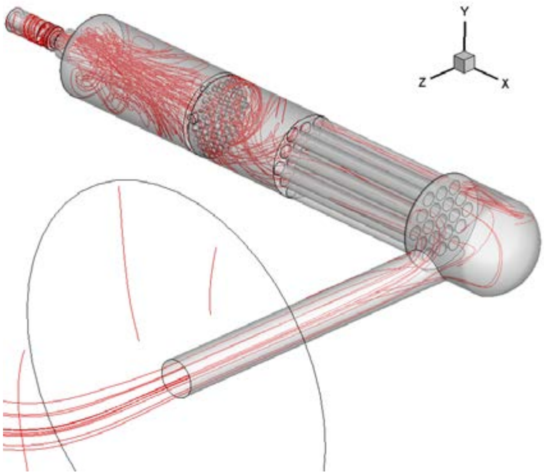


(d) using a vector wall (oxygen-rich supply)

Fig. 15. Stream traces for the SRU thermal reactors using a choke ring or a spiral-type vector wall (Yeh, 2016b).

Table 4 shows the sulfur and NO concentrations at the exit. It can be seen that using an opposing-type vector wall, the exit sulfur concentrations are increased by 0.3% and 1.6% for the oxygen-normal and the oxygen-rich operations, respectively, while the exit NO concentrations are increased by 3.4% and 7.5% for the oxygen-normal and the oxygen-rich operations, respectively, in comparison with using a choke ring. On the other hand, using a spiral-type vector wall, the exit sulfur concentrations are increased by 4.3% and 4.7% for the oxygen-normal and the oxygen-rich operations, respectively, while the exit NO concentrations are increased by 14.4% and 16.3% for the oxygen-normal and the oxygen-rich operations, respectively, in comparison with using a choke ring. Among the choke ring and vector walls investigated, the spiral-type vector wall produces the highest sulfur and NO concentrations at the exit.

Table 4. Sulfur and NO concentrations at the exit using a choke ring or a vector wall.

(a) oxygen-normal supply

| | Exit sulfur concentration (mole fraction) | Exit NO concentration (ppm) |
|---|---|---|
| choke ring | 0.0791 | 1.18 |
| opposing-type vector wall | 0.0793 | 1.22 |
| spiral-type vector wall | 0.0825 | 1.35 |

(b) oxygen-rich supply

| | Exit sulfur concentration (mole fraction) | Exit NO concentration (ppm) |
|---|---|---|
| choke ring | 0.0902 | 14.7 |
| opposing-type vector wall | 0.0916 | 15.8 |
| spiral-type vector wall | 0.0944 | 17.1 |

## CONCLUSIONS

In this paper, nitric oxide produced by an industrial-scale SRU thermal reactor is analyzed. Both the prototype reactor and its modifications, including modifying the zone 1 corner geometry, modifying the choke ring, and using a vector wall, are compared to seek a feasible way of reducing NOx emission. Practical operating conditions from a petrochemical corporation in Taiwan were used as the design conditions for the discussion.

**Main Findings**

For the reactors investigated in this study, the following findings are obtained from the simulation results:

(1) The SRU thermal reactor with a radius of curvature 1m at the zone 1 corner has the lowest NO emission among the radii of curvature at the zone 1 corner investigated.

(2) Among the choke ring heights investigated, the SRU thermal reactor having a choke ring height of 1.11m has the highest NO emission while the one having a choke ring height of 0.74m has a lower NO emission.

(3) Among the choke ring positions investigated, the SRU thermal reactor having a choke ring away from the zone 1 corner by 6m has the lowest NO emission while the one having a choke ring away from the zone 1 corner by 3m has the highest NO emission.

(4) The NO concentration at the reactor exit using a vector wall is higher than that using a choke ring.

(5) Using an opposing-type vector wall, the exit NO concentrations are increased by 3.4% and 7.5% for the oxygen-normal and the oxygen-rich operations, respectively, in comparison with using a choke ring. Using a spiral-type vector wall, the exit NO concentrations are increased by 14.4% and 16.3% for the oxygen-normal and the oxygen-rich operations, respectively, in comparison with using a choke ring. Compared with a choke ring or an opposing-type vector wall, a spiral-type vector wall produces more NO at the exit.

(6) Among the SRU thermal reactors investigated in this study, the SRU thermal reactor using a choke ring of 0.74m in height and 6m away from the zone 1 corner is a feasible compromise among the sulfur production, the operating temperature (service life consideration) and the NO emission.

**Concluding Remarks**

In this research, we choose an industrial-scale SRU thermal reactor from a petrochemical corporation in Taiwan as our basic model for discussion because its operating conditions are available as the input data for numerical simulation. However, the results of this study are not only restricted to the above specified SRU, but also are valuable to the researchers who are interested in the SRU operated on the Clause process. In the design of a SRU thermal reactor, the sulfur recovery is of course the primary concern because this is the main function of a SRU. Further, influence of the operating temperature should not be underestimated in comparison with the sulfur recovery because it is closely connected with the service life of a SRU. Therefore, in the design of a low-NOx SRU, the sulfur recovery, the operating temperature and the NOx emission should be taken into account simultaneously. The optimal design is a compromise among these three factors. For example, the SRU thermal reactor without a choke ring has the lowest NO emission and sulfur recovery because of its lowest zone 1 temperature. However, it has the highest zone 2 temperature and this is harmful to the downstream heat exchanger pipes. Although a vector wall produces more sulfur, its NO emission is also higher because of its higher operating temperature, which might be harmful to the reactor. Our experience of using a vector wall in Taiwan showed that the high temperature may damage the zone 1 corner. In summary, to determine a suitable design, a detailed numerical simulation should be performed first to find the sulfur recovery, the operating temperature and the NOx emission. The optimal design is a compromise among these three factors. Finally, in addition to the prototype reactor and its modifications (including modifying the zone 1 corner geometry, modifying the choke ring, and using a vector wall) investigated in this paper, the author has discussed other factors influencing the NOx emission of a SRU thermal reactor, including changing fuel mass fraction, changing inlet air quantity, changing inlet oxygen mole fraction, and changing burner geometry. The interested readers are referred to reference (Yeh, 2017) for detail.

## ACKNOWLEDGMENT

This research is funded by the Ministry of Science and Technology, Taiwan, under the contract MOST107-2221-E-150-012. The author is also grateful to the Formosa Petrochemical Corporation in Taiwan for providing valuable data and constructive suggestions to this research during the execution of the industry-university cooperative research project under the contract 104AF-86.

## REFERENCES

Adewale, R., Salem, D.J., Berrouk, A.S., and Dara, S., “Simulation of Hydrogen Production from Thermal Decomposition of Hydrogen Sulfide in Sulfur Recovery Units,” *J. Clean Prod.*, Vol.112, No.5, pp.4815-4825 (2016).

Chardonneaua, M., Ibrahim, S., Gupta, A.K., and AlShoaibi, A., “Role of Toluene and Carbon Dioxide on Sulfur Recovery Efficiency in a Claus Process,” *Energy Procedia*, Vol.75, pp.3071-3075 (2015).

Franco, A. and Diaz, A.R., “The Future Challenges for “Clean Coal Technologies”: Joining Efficiency Increase and Pollutant Emission Control,” *Energy*, Vol.34, No.3, pp.348-354 (2009).

Hassan, G., Pourkashanian, M., Ingham, D., Ma, L., and Taylor, S., “Reduction in Pollutants Emissions from Domestic Boilers—Computational Fluid Dynamics Study,” *J. Therm. Sci. Eng. Appl.*, Vol.1, 011007 (2009).

Javed, M.T., Irfana, N., and Gibbs, B.M., “Control of Combustion-Generated Nitrogen Oxides by Selective Non-Catalytic Reduction,” *J. Environ. Manage.*, Vol.83, No.3, pp.251-289 (2007).

Launder, B.E. and Spalding, D.B., *Lectures in Mathematical Models of Turbulence*, Academic Press, London, England (1972).

Launder, B.E. and Spalding, D.B., “The Numerical Computation of Turbulent Flows,” *Comput. Method App. M.*, Vol.3, No.2, pp.269-289 (1974).

Monnery, W.D., Hawboldt, K.A., Pollock, A., and Svrcek, W.Y., “New Experimental Data and Kinetic Rate Expression for the Claus Reaction,” *Chem. Eng. Sci.*, Vol.55, No.21, pp.5141-5148 (2000).

Normann, F., Anderson, K., Leckner, B., and Johnson, F., “Emission Control of Nitrogen Oxides in the Oxy-Fuel Process,” *Prog. Energy Combust. Sci.*, Vol.35, No.5, pp.385-397 (2009).

Patankar, S.V., *Numerical Heat Transfer and Fluid Flows*, McGraw-Hill: New York, USA (1980).

Selim, H., Gupta, A.K., and AlShoaibi, A., “Effect of Reaction Parameters on the Quality of Captured Sulfur in Claus Process,” *Appl. Energ.*, Vol.104, pp.772-776 (2013).

Shin, M.S., Kim, H.S., Jang D.S., “Numerical Study on the SNCR Application of Space-Limited Industrial Boiler,” *Appl. Therm. Eng.*, Vol.27, No.17-18, pp.2850-2857 (2007).

Siegel, R. and Howell, J.R., *Thermal Radiation Heat Transfer*, Hemisphere Publishing Corporation, Washington DC, USA (1992).

Sivathanu, Y.R. and Faeth, G.M., “Generalized State Relationships for Scalar Properties in Non-Premixed Hydrocarbon/Air Flames,” *Combust. Flame*, Vol.82, pp.211-230 (1990).

Yeh, C. L., “Numerical Analysis of the Combustion and Fluid Flow in a Carbon Monoxide Boiler,” *Int. J. Heat Mass Tran.*, Vol.59, pp.172-190 (2013).

Yeh, C. L., “Effect of Choke Ring Position on Thermal and Fluid Flow in a SRU Thermal Reactor,” *Int. J. Mech. Eng. Robot Res.*, Vol.4, No.3, pp.273-277 (2015).

Yeh, C. L., “The Effect of Fuel Mass Fraction on the Combustion and Fluid Flow in a Sulfur Recovery

Unit Thermal Reactor," *Appl. Sci.*, Vol.6, No.11, 331, DOI:10.3390/app6110331 (2016a).

Yeh, C. L., "Numerical Analysis of the Effects of Streamlining Geometry and a Vector Wall on the Thermal and Fluid Flow in a SRU Thermal Reactor," *Trans. Can. Soc. Mech. Eng.*, Vol.40, No.5, pp.811-820 (2016b).

Yeh, C. L., "Effect of Choke Ring Dimension on Thermal and Fluid Flow in a SRU Thermal Reactor," *Trans. Can. Soc. Mech. Eng.*, Vol.40, No.4, pp.511-520 (2016c).

Yeh, C. L., "NOx Pollution Analysis for a Sulfur Recovery Unit Thermal Reactor," *IOP Conf. Ser.: Mater. Sci. Eng.*, Vol.282, 012020 (2017).

Yeh, C. L. and Chien, T. C., "Effect of a Vector Wall on the Thermal Field in a SRU Thermal Reactor," *Int. J. Mater. Mech. Manuf.*, Vol.6, No.4, pp.243-249 (2018).

## NOMENCLATURE

| | |
|---|---|
| $C_{\mu}$ | turbulence model constant (=0.09) |
| $k$ | turbulence kinetic energy ($m^2/s^2$) |
| L | hydraulic diameter (m) |
| $l$ | characteristic length (m) |
| P | pressure ($N/m^2$) |
| T | temperature (K) |
| V | velocity (m/sec) |
| XYZ | cartesian coordinates (m) |
| $x$ | mole fraction (%) |
| $\varepsilon$ | turbulence dissipation rate ($m^2/s^3$) |

# 具流線化轉角、阻氣環或向量壁之硫回收單元熱反應爐氮氧化物生成數值研究

葉俊郎
國立虎尾科技大學飛機工程系

## 摘 要

本文旨在針對硫回收單元熱反應爐內部流場進行詳細的數值模擬，並進行汙染分析，以期提升其操作效能並避免過度的汙染排放，探討內容包含以下三項因素對於氮氧化物生成之影響：(1)反應爐幾何形狀之影響、(2)阻氣環之影響、(3)向量壁之影響。由研究結果發現，在反應爐第一區轉角流線化方面，當流線化曲率半徑為 1m 時，出口一氧化氮濃度最低。在阻氣環高度方面，當阻氣環高度為 1.11m 時，出口一氧化氮濃度最高，而當阻氣環高度為 0.74m 時，其出口一氧化氮濃度較低。在阻氣環位置方面，當阻氣環位於第一區轉角下游 6m 處時，出口一氧化氮濃度最低，在另一方面，當阻氣環位於第一區轉角下游 3m 處時，出口一氧化氮濃度最高。使用向量壁比使用阻氣環之硫回收單元熱反應爐出口一氧化氮濃度高。在本研究所探討之熱反應爐中，當無阻氣環時，出口一氧化氮濃度最低，然而，其第二區溫度最高，這對於下游的熱交換管有害。雖然向量壁可產生較多的硫，但其一氧化氮排放濃度亦較高。綜合來看，考量硫的產量、流場溫度(與使用壽命相關)、以及一氧化氮排放量等因素，具有高度 0.74m、且位於第一區轉角下游 6m 處阻氣環之硫回收單元熱反應爐為最佳設計。